

STUDY ON THE CORROSION RESISTANCE CHARACTERISTICS OF N-TiO₂/Al₂O₃ REINFORCED HYBRID Mg COMPOSITES

V.K NEELA MURALI ^{1*} AND M.S STARVIN ²

¹Department of Mechanical Engineering, Ponjesly College of Engineering, Nagercoil, TN, India.

²Department of Mechanical Engineering, University College of Engineering, Nagercoil, Konam, Nagercoil, TN, India.

ABSTRACT

The Mg based composites with the element addition of 3Zn, 0.5Mn and the reinforcement of ceramic particles nanoTiO₂ and Al₂O₃ are added to form an Mg- hybrid composites through powder metallurgy method. The examination is mainly concentrated on the effect of multi ceramic particles such as nanoTiO₂ and Al₂O₃ inclusion in the composite matrix for the characteristics of hardness, tensile strength, wear and corrosion. Optical and scanning electron microscopy are used for the micro structural variation. X-ray diffraction is used to analysis the various phases available in the hybrid composites matrix. Many intermetallic phase are formed during heat treatment process which reduces the porosity and increases density and corrosion resistance of the composites. The hard ceramic particles inclusion, hot extrusion process and heat treatment or stress-relieving mechanism enhances the above said properties of the prepared hybrid composites.

Keywords: Chemical properties, Hardness, Heat treatment, Microstructure, Mg based composite, Reinforcement.

1. INTRODUCTION

The composites are formed by two or more materials are combined together to enhanced the physical, mechanical and chemical properties over the individual materials. In general, the strength of composite material formation is depends with the reinforcement of metal/material into the composite matrix [1]. Now-a-days, composites are formed for using aerospace, sporting goods, military equipment and engineering and bio-medical structures. These applications are requires light weight with high strength and better machinability with damping characteristics. Recently, after iron and aluminum, magnesium (Mg) is widely used in mentioned applications. Because magnesium and its alloys and composites are possessing the above said properties. In contrast, the magnesium's applications are limited in the field which requires high elastic modulus, hardness and electricity [2].

A various characteristics of the magnesium can be enhanced by forming alloys and composites through proper selection of alloying elements and particle reinforcements respectively which can be further improved by heat treatment or stress relieving process [3]. The alloying elements and the reinforced particles are forming different secondary phases in the matrix during heat treatment. The secondary phase formation is depends with the nature of added elements and their chemical reactivity with the matrix material. The formed secondary phases could be improved the interfacing strength of the matrix material [4, 5]. In light weight material application, Mg alloys and their composites are exhibits satisfied mechanical properties.

Other than magnesium, aluminum (Al) matrix composites are also used in light weight engineering applications. Many researchers are giving attention to use Al matrix based alloys and composites in industrial applications [6, 7]. Similarly, titanium (Ti) based alloys are also utilized in various engineering applications. The density of the magnesium alloys are compared to aluminum and titanium alloys, its densities are approximately 35% and 65% lesser respectively [8]. The researchers suggested that the density range of magnesium alloys are lies between 1.74 and 2 gm/cm³. This range is similar to the human bone density. Therefore, the magnesium alloys and their composites are useful for biomedical applications [9, 10]. The melting temperature of the magnesium is lower than the other widely used materials such as iron, aluminum and titanium as around 654 °C [10] and the manufacturing and maintenance cost of the magnesium products are very much lesser as compared to Al and Ti based alloys and composites [11]. The Magnesium alloys are having lower young's modulus but this can be enhanced by the addition of ceramic hard particles as reinforcements [12]. The economy and suitability for forming concern of the Mg composites, most of the researchers are concentrates their research work in the field of structural, biodegradable and biomaterials for human body implants [2, 11, 13 - 15].

In-general, the most of the studies are focusing the Mg composites based on their characteristics improvement through element addition by varying their grain size, weight percentage, morphology, reinforcement particles distribution and by altering the composites forming techniques [16-18]. Recent years, several alloys and composites are developed using titanium oxide (TiO₂) as the

reinforcement in Mg matrix through powder metallurgy methods [3, 19, 20]. The added TiO₂ reinforcements improved the strength of the composites than the pure form of Mg metal. A hot extrusion process is highly enhanced the characteristics of the composites prepared through powder metallurgy method (PM) by altering the microstructure of the elements present in the composites [15]. The microstructural alteration process tends to form a new inter-metallic phases. This can be done through recrystallization of grains and precipitation of the same occurring during hot extrusion process. Al₂O₃ is one of the reinforced element for the Mg composites and is bio-degradable [21]. This element addition in Mg alloy is enhanced its physical and mechanical characteristics [22-25]. Similarly, this element reinforcement in Mg composites (AZ81 base) exhibits possible improvements in tensile and compressive characteristics when comparing AZ81 base alloy [26].

Generally, magnesium is a soft metal and having lower wear resistance therefore its application in wear characteristics field is limited [27]. The wear resistance characteristics of the magnesium is possible to improve through the addition of reinforced metal particles to form an Mg metal matrix composites. The various reinforcement materials are added to improve the wear characteristics Mg composites are SiC, Al₂O₃, fly ash, titanium carbides, nitrides and oxides and CNT's [28 - 30]. Moreover, the corrosion resistance of the pure form of Mg and its alloys are poor [31]. Because, the formation of alloys are creating intermetallic second phases at the grain boundaries causing negative polarization with the interior grains thus enhancing galvanic corrosion [32-34]. In-contrast, the addition of Al, Zn, Mn, Sn, Ca are enhances the corrosion properties of the Mg alloys and composites [35]. However, the requirement of Mg based alloys and composites applications are yet to be fulfilled.

The facts for the preparation of Mg matrix composites are depends with the selection of suitable reinforcement materials added into the Mg matrix. The selected reinforcement material should have (i) high mechanical strength and (ii) biocompatible and have good corrosion resistance [36, 37]. This work is to prepare and studied the Mg-3Zn-0.5Mn alloy and the reinforcement nanoTiO₂ and Al₂O₃ micro particulates added hybrid composites. The selected Mg matrix elements and reinforcement elements are biodegradable and are having good mechanical strength. The physical, mechanical and corrosion characteristics of the prepared alloys and the composites are investigated by its as-extruded and heat treated condition. The obtained results are discussed.

2. EXPERIMENTAL PROCEDURE

The composite elements are of 200 mesh is chosen for preparing an Mg-composites. The elements added to form an Mg-alloy is Mg, Zn, and Mn metal powders in micron level as 200 mesh. The physical properties of the alloying elements are given in the table 1. Similarly, the ceramic reinforcements are n-TiO₂ with the grain size 50 – 100 nm and the Al₂O₃ powders are in micron level. The Zn and Mn metal powders added to the matrix by 3wt% and 0.5 wt%. Similarly, the reinforcement of TiO₂ is as 0.1wt% and the Al₂O₃ added is varied by 1 wt% and 2 wt%. The elements are mixed thoroughly according to their respective weight at 350 rpm for 1 hour to form a 50mm diameter and 30mm

height sizes billet using powder metallurgy technique. The compacting pressure used for this purpose is 690Mpa and a specially attached hydraulic power press is utilized.

Table 1: Properties of monolithic metals for alloys [38]. Boyer & Gall. (1985))

Property	Mg	Zn	Mn
Density (g/Cm3)	1.74	7.14	7.21
Melting point (°C)	650	419.5	1246
Young's modulus (GPa)	45	108	180 – 190
Shear modulus (GPa)	17	43	74
Poisson ratio	0.29	0.25	0.23
Brinell hardness (MPa)	44-260	327-412	1800
Thermal expansion (10-6/K)	24.8	30.2	21

After the formed billets are sintered using 400°C temperature maintained in an argon environment for one hour. The secondary strengthening process is done on the billets through hot extrusion. The hot extrusion process is carried out 400°C temperature with 5.4:1 ratio and the extrusion speed maintained as 0.2 to 0.5 mm/s. After hot extrusion, the formed rods are heat treated to relieve the stresses. The heat treatment process is done at 260°C temperature for 20 minutes in argon atmosphere using electric muffle furnace with a heating rate of 20°/min is manufactured by 'Hasthas' Scientific Instrument Pvt. Ltd, Chennai, India. The prepared alloys and hybrid composites characteristics are examined at its as-extruded and heat treated or after stress relieving conditions.

The micro structural characteristic study is done through optical microscope (OM) and scanning electron microscope (SEM). The OM used for this purpose is MVHD-1000 AP/MP, Shanghoui Dahens Optics and Fine Mechanics Co. Ltd. A digital micro hardness tester is attached to this machine. Before capturing the image, the samples are etched through etchant. The etchant used for this study contains: picric acid:1.5 grams, ethanol: 25 ml, acetic acid: 10 ml are added in 10 ml distilled water. After completing the etching process, the samples are cleaned distilled water.

The wear characteristics of the hybrid composites are valued using a Pin-on-disc wear tester, manufactured by magnum engineers, India, Pvt. Ltd., The sliding speed 100 rpm, track radius 50 mm, running time 10 minutes and the applied load 10 N are used for the measurement. The disc is grounded finely with the silicon carbide paper sheet (Emery sheet) with the grit size 1200. A new sheet is used for every tested samples. After test, the samples are weighted using chemical digital balance. The specific wear rate is valued using the equations [39] and the specimen is prepared as per the ASTM standard G99 as 8mm diameter and 40 mm height.

$$\text{Specific wear Rate } W_s = \frac{\Delta m}{\rho t V_s F_n} \text{ mm}^3/\text{N-m} \quad \dots\dots\dots(1)$$

The equation (1) implies,

Δm – Specimen weight loss during test (Initial weight – final weight) in g.

ρ – Density of the alloys and hybrid composite in g/mm^3

F_n - Average applied load on the test specimen in N

V_s - Sliding velocity in m/s.

t - Test conducting period in s

Corrosion behavior of the hybrid composite is analyzed using Electro chemical analyzer CHI-604D, CH Instruments, USA. The analyzer is manufactured with three cell electrode configuration i.e., working electrode is specimen, reference electrode is saturated calomel electrode and platinum metal is as a counter electrode. The corrosion medium used for this study is saline water which contains 3.5 wt. % of NaCl. The scan rate used for this study is 1 mV s^{-1} with the room temperature. The corrosion rate is calculating from tafel electrochemical measurement using the equation (2) [15].

$$\text{Corrosion rate (CR)} = \frac{3.28M}{n\rho} i_{corr} (\text{mm y}^{-1}) \quad \dots\dots\dots(2)$$

n =Quantity of free electrons involved for corrosion reaction

M =Atomic mass

ρ = Test specimens density

3. RESULTS AND DISCUSSION

3.1 Microstructure

The obtained morphological changes during sintering and hot extrusion process are represented in the figure 1. From the optical microgram, it is clear that the elements present in the matrix are uniformly distributed. Also, the Al_2O_3 powder distribution is spread over the entire micrographs which implies that the reinforcement particles are almost properly mixed into the alloy matrix. But, in some places voids, micro pores and cavities are present in the composites. This cavity formation may happened due to the lesser compaction pressure applied and stretching effect during the extrusion process. The cavities are reduced by the heat treatment or stress relieving process. There is a slight difference occurs between the increasing reinforcement content added into the matrix in terms of cavities as shown in the fig. 1 (b) and (c). The increasing reinforcements could be reduces the microspores and voids during hot extrusion.

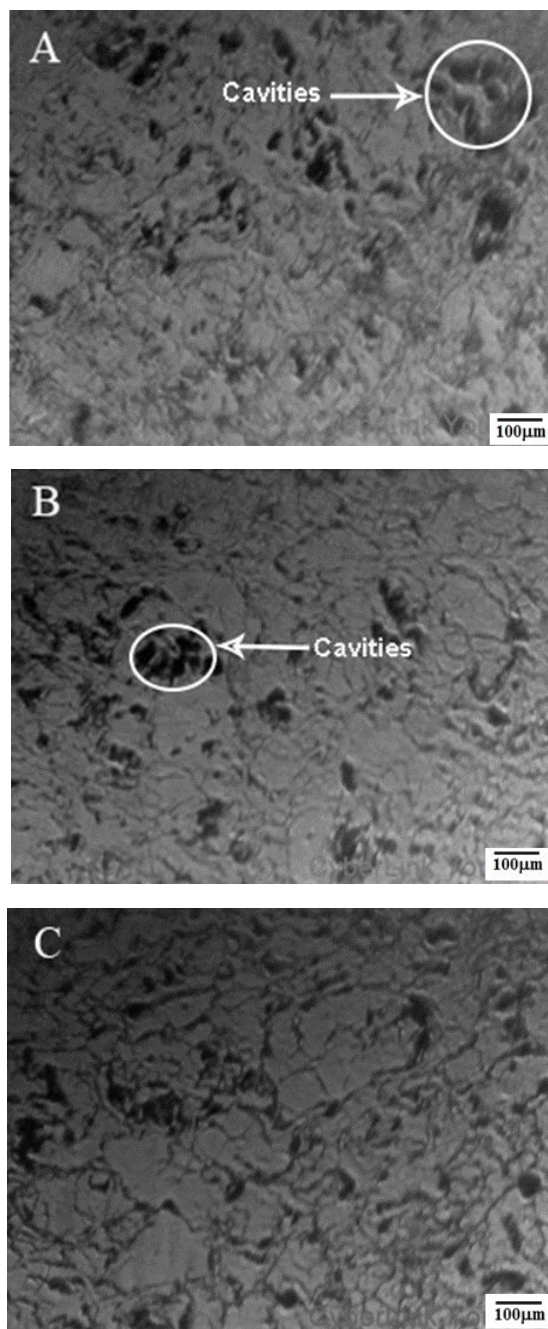


Figure 1. Optical microstructures of Mg hybrid composite: (a) as-extruded with 1% Al_2O_3 reinforcement (b) heat treated with 1% Al_2O_3 reinforcement (c) heat treated with 2% Al_2O_3 reinforcement.

The higher deformation could be occurred on the composite matrix due to hot extrusion process causing rearrangement of reinforcements. This rearrangement of reinforcements in the alloy matrix is filled the voids, cavities and pores present in the composite matrix [19]. The filled voids and pores leads to increase the bonding strength of the matrix due to interfacial reaction (Interfacial reaction is a physical attraction or molecular reaction happened between two different phases such as reinforcement and alloying elements can occur within the limits of the narrow interfacial region [40]) reinforcement and the alloy matrix [41]. The formed stretched grains are evident for the recrystallization taken place during sintering and hot extrusion process as shown in the fig.2(C). The formed grains are near equiaxed for after heat treatment than the as extruded as shown in the

fig. 2. The grain refinement is takes place to increase the sizes of the grains. The grain growth is mainly due to the ability of reinforcement n-TiO₂ and Al₂O₃ particles to nucleate the Mg-matrix during recrystallization process occurs at the heat treatment temperature between the temperatures (250°C - 400°C). And these particles are restricted the movement of the other alloying elements present in the composites causing grain pileup. In general, the addition of reinforcement of particles increases the grain boundaries of the composites. In contrast, the pileup of grains are increases its size by overlapping of grains thus reduces the number of grain boundaries. The reduction in grain boundaries enhanced the interfacial reaction between the matrix grains and reinforcement particles which leads to increase the bonding strength of the composites.

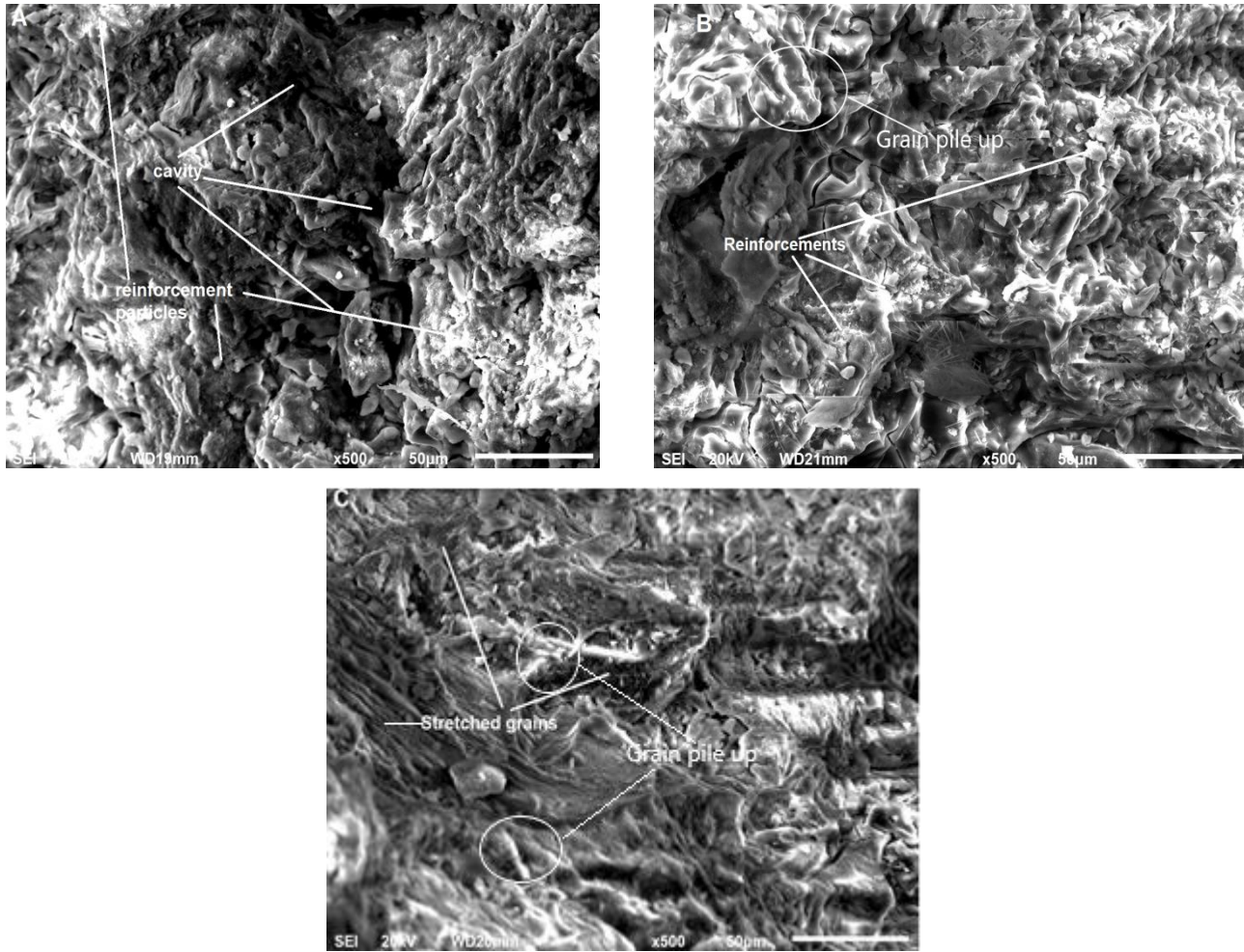


Figure 2. SEM of Mg composite (A) as-extruded Mg- hybrid composite with 2% Al₂O₃ (B) heat treated Mg-hybrid composite with 1% Al₂O₃ (C) heat treated Mg- hybrid composite with 2% Al₂O₃.

3.2 Porosity and Density

When comparing the figures. 2 (A), (B) and (C), it is clear that the heat treatment process decreases the cavities formed during the hybrid composite formation through powder metallurgy method. The reducing order of cavities are visible in the figures 2(C) and (B) respectively by increasing reinforcement

particles. The Archimedes principle is the easiest method to find the porosity and density of the composites [19]. In this work, the same method is used to calculate porosity and density of the composites. The distilled water is used as an immersion fluid for the porosity measurement. A digital type physical balance is used to measure the weight of the samples. The obtained density and porosity of the composites are depicted in the table.2.

Table 2. Density and porosity of Mg-composites

Specimen	Condition	Density (g/cm ³)	Porosity (%)
Mg-3Zn-0.5Mn without reinforcement	As-extruded	1.7246	37
Mg-3Zn-0.5Mn without reinforcement	Heat treated	1.7334	35
Mg-composite with n-TiO ₂ and 1% Al ₂ O ₃ reinforcement	As-extruded	1.7602	34
Mg-composite with n-TiO ₂ and 1% Al ₂ O ₃ reinforcement	Heat treated	1.7695	32
Mg-composite with n-TiO ₂ and 2 % Al ₂ O ₃ reinforcement	As-extruded	1.7921	31
Mg-composite with n-TiO ₂ and 2 % Al ₂ O ₃ reinforcement	Heat treated	1.8412	28

The density and porosity measurement reveals that, a noticeable reduction in the porosity obtained by the addition of reinforcement causing increase in density of the composites. From the table 1 it is clear that the heat treatment process could further rises the density of the composites. The decreasing porosity is due

to the release of entrapped gases present inside the composite during composite formation and the formed voids and pores are filled during heat treatment process. During heat treatment, oxidation of Mg might to be happened is the other reason for reducing porosity and increasing density of the composites.

Table 3. Micro hardness value of Mg and Mg-composites

Materials	Condition	Average micro hardness (VHV)
Pure Mg	Pure form	48
Mg-3Zn-0.5Mn/0.1TiO ₂	Before heat treatment	69
Mg-3Zn-0.5Mn/0.1TiO ₂	Heat treated	72
Mg-3Zn-0.5Mn/0.1TiO ₂ /1Al ₂ O ₃	Before heat treatment	76
Mg-3Zn-0.5Mn/0.1TiO ₂ /1Al ₂ O ₃	Heat treated	81
Mg-3Zn-0.5Mn/0.1TiO ₂ /2Al ₂ O ₃	Before heat treatment	84
Mg-3Zn-0.5Mn/0.1TiO ₂ /2Al ₂ O ₃	Heat treated	92

3.3 Hardness

The Vickers micro hardness value (VHV) of the pure Mg and Mg- hybrid composites are evaluated through the digital Vickers micro-hardness tester using a pyramidal diamond indenter. The specification of the micro-hardness test is 136° included angle, 25g indenting load and 20s as dwell time. The obtained results are depicted in the table 3. The pure Mg exhibits lower micro hardness when compared to all the prepared Mg- hybrid composites. This could be due to the addition of reinforcements. The increasing quantity of reinforcement addition can further increases the hardness value of the composites. Moreover, the heat treated hybrid composite are exhibits a highest hardness than their as extruded condition. The addition of TiO₂ and Al₂O₃ particles are having higher hardness value than the Mg causing hardness improvement in the hybrid composites. The addition of TiO₂ reinforcement is very much lesser as compared to the other elements present in the hybrid composites. Therefore, the n-TiO₂ elements are not much effected for the enhancement of micro hardness value of the hybrid composites when compared to the higher quantity addition of Al₂O₃ particles.

Other than the hard ceramic particles inclusion, hot extrusion and heat treatment process plays a major role for increasing the hardness of the composites. The hot extrusion process is execute a recrystallization of grains in dynamic manner and precipitate the grains which are enhances the hardness of the composites. The heat treatment after hot extrusion process refines the grains. The refining of grains are depends with the temperature used for the heat treatment process. The melting temperature of the titanium is higher than all the other elements present in this hybrid composite. Therefore, there is no recrystallization or grain refining benefit is gathered from the TiO₂ particles inclusion.

The grains of the Mg- composites are evaluated through X-ray diffraction (XRD) using a Siemens X-ray diffractometer with Cu-K α radiation. Phases formed in the composites are obtained from the diffractograms. The scanning angles (2 θ) with a step size of 0.02° per 2 s is used for this purpose. The obtained XRD is depicted in the fig .3. The mentioned figure revealed the available phases of the composites. Some of the intermetallic phases such as MgO, Mn₂O₃, Mg₂Zn₃, Ti₂Al etc., are shown in the XRD along with the primary phases Mg, TiO₂, Al₂O₃. These formed intermetallic phases are also possible to fill the micro voids causing hardness improvement.

Table 3: Tensile Characteristics of Hybrid Composites

Material	Ultimate Tensile Strength (MPa)	Yield Strength (MPa)	Fracture Strain (%)
Mg-3Zn-0.5Mn/0.1TiO ₂ /1Al ₂ O ₃ hybrid composite (as-extruded)	222.52±3	146.51±2	5.96±2
Mg-3Zn-0.5Mn/0.1TiO ₂ /1Al ₂ O ₃ hybrid composite (heat treated)	225.33±3	131.48±2	6.78±1
Mg-3Zn-0.5Mn/0.1TiO ₂ /2Al ₂ O ₃ hybrid composite (as-extruded)	250.94±3	159.48±2	8.82±1
Mg-3Zn-0.5Mn/0.1TiO ₂ /2Al ₂ O ₃ hybrid composite (heat treated)	259.12±4	196.06±2	18.78±2

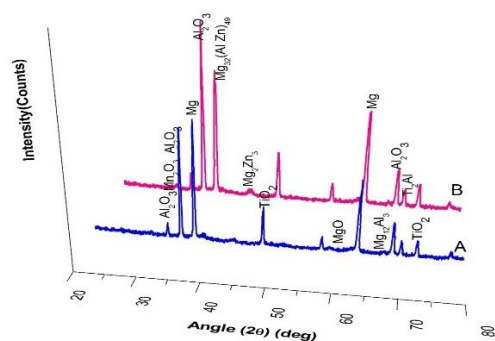


Figure 3. X-ray diffraction of heat treated Mg-hybrid composites (A) 1% Al₂O₃ and (B) 2% Al₂O₃.

3.4 Tensile Strength

The tensile strength of the composites are calculated using DAK-UTB9103 computerized mechanical testing machine at room temperature. The movement of the crosshead was maintained at 0.25 mm/min. The obtained results for the as-extruded and stress relieved Mg-3Zn-0.5Mn alloys and n-TiO₂ and Al₂O₃ reinforced hybrid composites are tabulated in the Table 3 and the corresponding test resulted graphs are depicted in the figure 4. The test results indicates that the maximum ultimate tensile strength (259.12 MPa), fracture strain (18.78%) both the values are higher than Muhammad et. al., (2015) [42] values and the yield strength (196.06) is obtained for the heat treated Mg hybrid composites. All the obtained tensile properties values of the composites are higher than that of pure magnesium metal in as-extruded condition is 178 MPa.

The tensile property enhancement for the hybrid composites are governed by the proper distribution of ceramic particles such as TiO₂ and Al₂O₃ with the Mg matrix. The reinforced particles increases the area of the grain boundary thus improves the surface integrity between the matrix phases and the reinforcement phases. Also, the hot extrusion process causing dislocation movements. The dislocation movements are arrested by these reinforcements causing buildup of dislocations. The dislocation pile-ups are occurred at the grain boundaries. This dislocation pile-ups are causing cavitation at the grain boundaries leads to reduce the tensile properties of the composites [43].

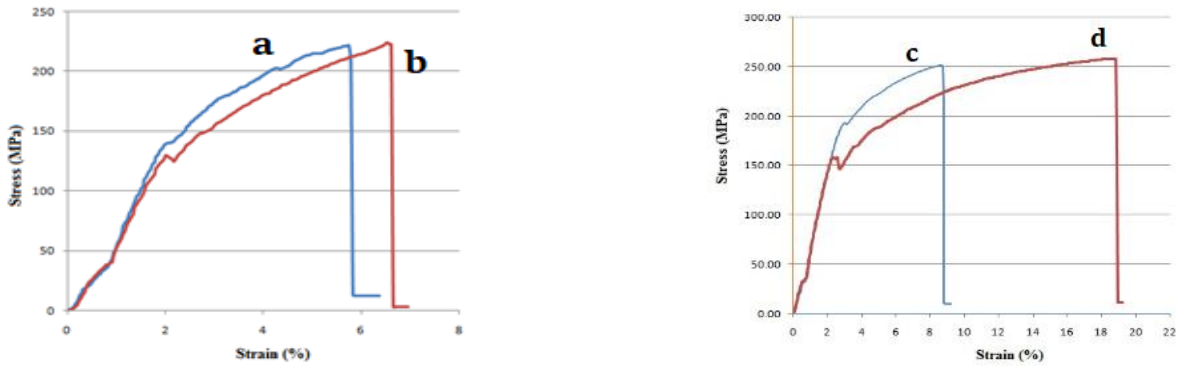


Figure 4. Tensile test curves (a) Mg-3Zn-0.5Mn/0.1TiO₂ composite (as-extruded) (b) Mg-3Zn- 0.5Mn/0.1TiO₂ composite (heat treated) (c) Mg-3Zn-0.5Mn/0.1TiO₂/1Al₂O₃ hybrid composite (as-extruded) (d) Mg-3Zn-0.5Mn/0.1TiO₂/2Al₂O₃ hybrid composite (heat treated).

It is reported that the heat treatment process has a vital influence on the tensile characteristics Mg alloys and composites [44]. The dislocation pile-ups mentioned above at the grain boundaries of the hybrid composites, which resists the elongation of the material upon tensile loading. When the as-extruded and heat treated hybrid composites are compared, the heat treated hybrid composites are having higher fracture strain. This may be due to the reduction of the following: size of the cavities, number of pores and voids formed during

manufacturing process after heat treatment process. Commonly, the tensile loading can strain the composite and the strained effect is shifted to the reinforced particles through shear stresses which resist the deformation against fracture. But, the rupture efficiency of the composite is depends with the distribution of reinforcement particles, interfacial bonding between the reinforcement particles and matrix elements, volume fractions of reinforcement addition etc., [45].

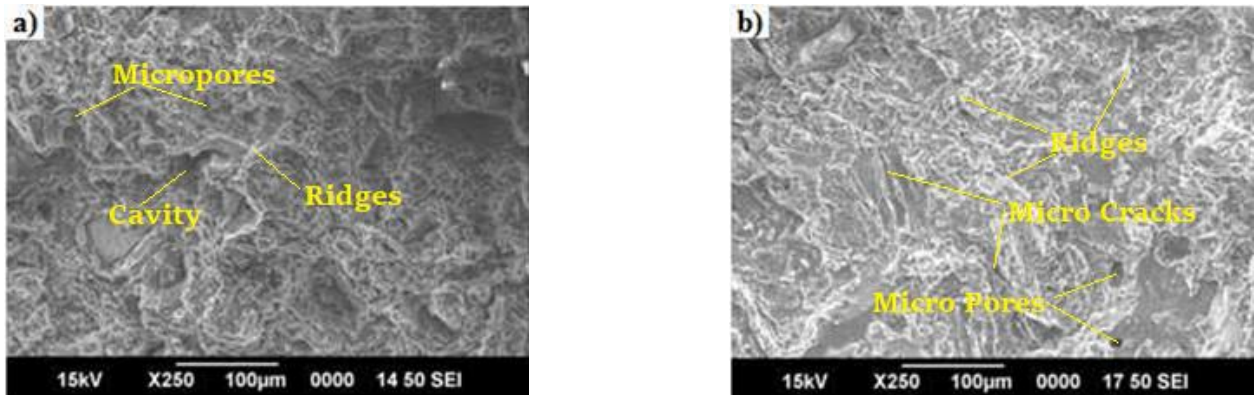


Figure 5. Scanning electron micrographs of hybrid composites after tensile test (a) As-extruded hybrid composite (b) heat treated hybrid composites.

The homogenous distribution of the particles with limited porosity and grain refinement may influenced the improvement in fracture strain. The homogenous distribution of the reinforcements reduces the stress concentration along with the alloy matrix. The reinforcement in the dispersed form across the matrix provides sites for cleavage steps and fractures tends to improve the tensile strength of the composite. The surfaces after tensile test is depicted in the figure 5. It reveals that, dimples and ridges are present in the tensile fracture facades. The presence of dimples and ridges are indicates that, the occurred fracture may due to ductile fracture. The increased quantity of reinforcement in the hybrid composite is shallower the dimples on the entire matrix as evident from the figure 5. The fracture surfaces contain cleavage fracture steps, micro-cracks, microspores, and coarse intermetallic phases. The propagation of the micro cracks is obstructed by the coarse intermetallic phases and the formed dislocation pile-ups at the grain boundaries. The dimple formation shows the non-basal slip system is triggered during tensile loading. The non-basal slip system may improve the tensile strength of the hybrid composites.

3.5 Wear Strength

The specific wear rate of the Mg-hybrid composite is calculated using the equation.1. The velocity of sliding is maintained constant as 0.4 m/s. The obtained results are depicted in the figure. 6. The specific wear rate of the as-extruded hybrid composites are higher than the heat treated hybrid composites. This could be due to the high amorphous or porous nature of the as-extruded hybrid composites. The stress relieving or heat treatment process might be converting the amorphous nature of the hybrid composite into crystalline nature. Also, the as-extruded composites yields lower hardness than the heat treated composites as mentioned earlier. The increasing addition of Al₂O₃ reinforcement

into the matrix improved the wear resistance of the hybrid composites. Similar result is reported by Mahadi et. al., (2018) [46] and Thirugnana et. al., (2019) [47]. The obtained results shown that the increasing reinforcement addition is increases the hardness value of the hybrid composites by reducing porosity. The added n-TiO₂ particles are filled the gap between the grain boundaries formed by composites elements. Generally, the hardness and wear resistance are directly proportional thus improves the wear resistance of the as-extruded hybrid composites.

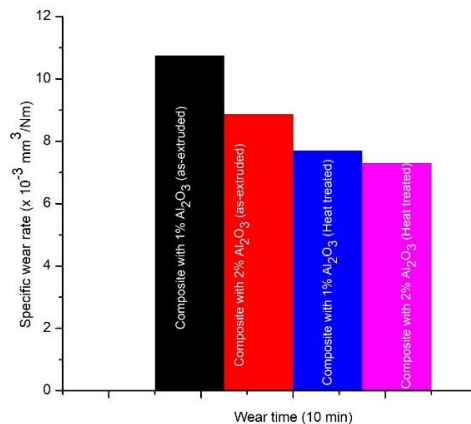


Figure 6. Wear rate of the Mg-3Zn-0.5Mn alloy with 0.1 wt. % of TiO₂ and varying wt. % of Al₂O₃ particles reinforced hybrid composites.

From the figure. 6, it is clear that the heat treatment process enhances the wear resistance of the hybrid composites. This could be due to the following: (i) increasing wettability of Al_2O_3 and TiO_2 reinforcement particles and (ii) grain refinement due to recrystallization of the matrix elements. Both the factors are causing the formation of intermetallic bond between reinforcements and matrix elements. The formation of intermetallic bonds are evident for the formation of second metallic phases such as $\text{Mg}_{12}\text{Al}_3$, Ti_2Al , $\text{Al}_2\text{O}_3\text{Mn}_2\text{O}_3$ etc., as shown in the figure. 3 and are discussed earlier in the hardness property section.

The worn surface morphology is depicted in the fig. 7, it shows that the abrasive and adhesion wear characteristics are the predominant wear mode occurred on the hybrid composites. In some places, scratch markings are visible which shows that the pull out particles comes out from the reinforcement and the SiC emery paper sheet struck in between the sliding surface to make this markings. And these pull out particles are gain heat due to friction by continuous sliding causing oxide formation. The formed oxides are acts as a protective layer to avoiding direct contact between the sliding surfaces [48] thus improves the wear resistance of the hybrid composites.

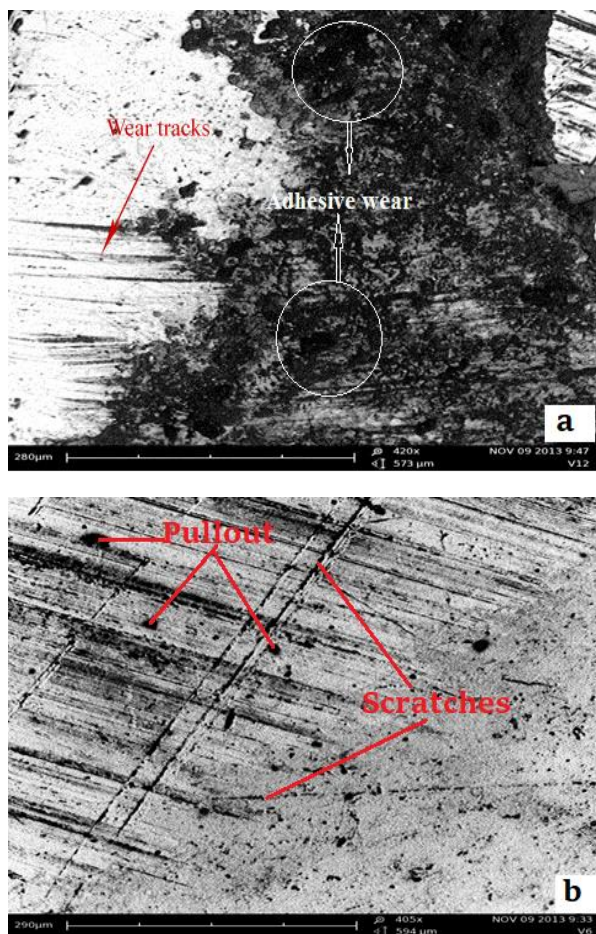


Figure 7. SEM images of worn surface morphologies (a) Mg-3Zn-0.5Mn/0.1TiO₂/1Al₂O₃ hybrid composite (as-extruded) (b) Mg-3Zn-0.5Mn/TiO₂/2Al₂O₃ hybrid composite (heat treated).

3.6 Corrosion characteristics

Limited corrosion performance of the magnesium and its alloys are the major bottleneck in widespread usage of the same materials. But it can be enhanced by adding reinforcement to making composites and surface modification technologies [49]. The selected reinforcement's n-TiO₂ and Al₂O₃ are having acceptable corrosion performance than the pure magnesium. The tafel plot for the prepared Magnesium alloys and its hybrid composites are depicted in the figure 8 and the obtained corrosion rate values of the same are plotted in the figure 9. From the mentioned figures 8 and 9, it is clear that, the heat treated alloy and the hybrid composites are exhibits higher corrosion resistance than its as-extruded condition.

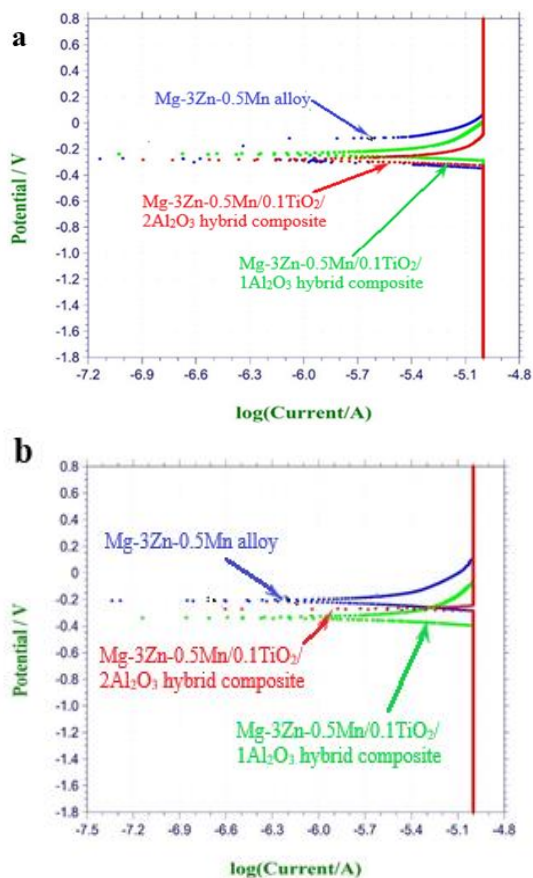


Figure 8. Electrochemical polarization curves (a) as-extruded alloy and hybrid composites (b) heat treated alloy and hybrid composites

Moreover, the prepared Mg-alloys with their as-extruded and heat treated condition yields lower corrosion resistance when compared with all the conditions of hybrid composites. This could be due to the higher porosity having the alloys than the hybrid composites. The porous nature of the alloy having more numbers of cavities which allows the corrosion medium can penetrate inside the alloy matrix causing the formation of more corrosion sites. This increasing corrosion sites are leads to enhance the corrosion reaction thus reduce the corrosion performance of the alloy system. The hybrid composites are having lesser porosity than the alloy system therefore the presence of number of cavities are lesser than the alloy system. The reduced cavities are improved the corrosion performance of the hybrid composites.

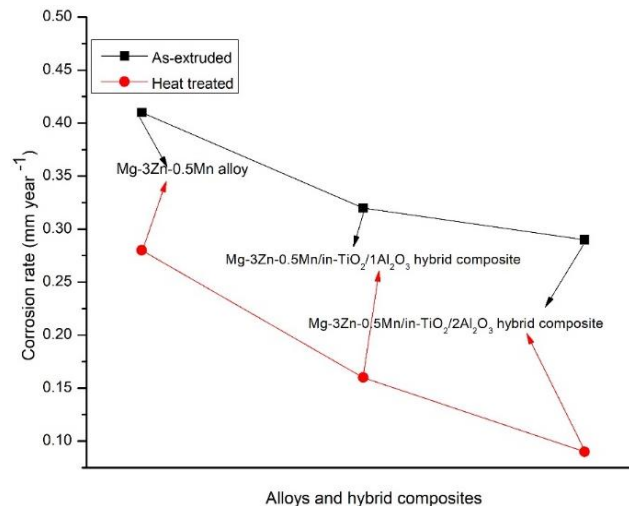


Figure 9. Corrosion performance of Mg-alloy and hybrid composites.

The slope of corrosion rate curves implies that the improvement in corrosion is higher for the heat treated hybrid composites than the as-extruded hybrid composites. Also, this improvement is higher for the increased content of Al₂O₃ hybrid composites. This could be due to the grain refinement occurs at the grain boundaries by the formation of second phases such as Mg₂Zn₃ and this formed phases improved the density of composites [50]. During corrosion process, the individual grains or particles are reacts with the corrosion medium and pulled off from their places but it can arrested by the addition lesser particle sizes [51]. The added n-TiO₂ particles can filled the gap of the grain boundaries by the process of hot extrusion and after heat treatment which are not much affected by the corrosion medium due to its inertness. This may be the reason for increasing corrosion resistance of the heat treated hybrid composites.

During corrosion, the magnesium alloys and composites are forming magnesium hydroxide film on the surfaces of Mg matrix which is slightly soluble in aqueous solution thus gives protection to corrosion reaction. The solubility of the protection layer depends with the reaction time and acceleration potential. The forming second phases are accelerate the corrosion reaction to destroy the magnesium oxide film causing localized corrosion. In contrast, the formed second phases and the added reinforcements are inert to aqueous solution causing uniform corrosion. The localized corrosion is reduced the corrosion performance of the Mg-alloys and its composites [52]. From the figure 10, it is evident that there is no localized corrosion behavior is taken place. Thus improved the corrosion resistance of the hybrid composites.

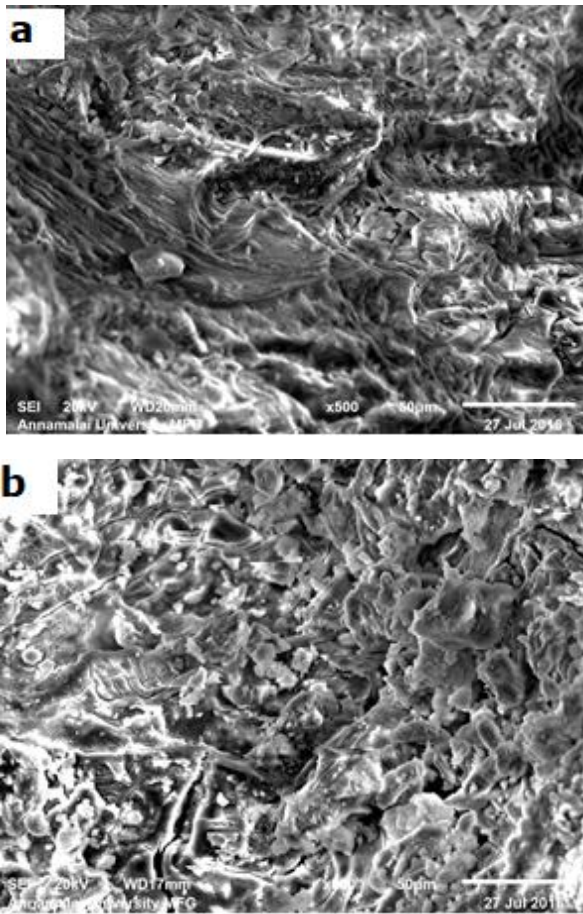


Figure 10. SEM images after corrosion for heat treated hybrid composites (a) Mg-3Zn-0.5Mn/0.1TiO₂/1Al₂O₃ (b) Mg-3Zn-0.5Mn/0.1TiO₂/2Al₂O₃.

CONCLUSIONS

- ✓ The uniformly distributed reinforced phase into the Mg matrix is to increases the surface integrity between both the phases leads to improve the strength of the composite. Hot extrusion and heat treatment process are enhances the harness characteristics of the composites through dynamic recrystallization and grain refinement.

- ✓ The reinforced TiO₂ and Al₂O₃ nanoparticles are arrest the dislocation movement leads to grains pileup yields to the increase in strength of the composites
- ✓ The refined grains after grain pile-ups are reduces the area of the grain boundary through reinforcement of n-TiO₂ and Al₂O₃ ceramic particles thus enhances the tensile strength of hybrid composites.
- ✓ The hard reinforcements, forming intermetallic second phases during hot extrusion and heat treatment process forming oxides from the debris during abrasion may improves the wear resistance of the hybrid composites.
- ✓ The corrosion performance is improved by reduction in porosity, chemically inert particles inclusion and the uniform corrosion.

REFERENCES

1. M. Edwin Sahayaraj, J.T. WinowlinJappes, I. Siva. *J. Adv. Microsc. Res.*, 9, 16-21, (2014).
2. P.N. Lim, R.N. Lam, Y.F. Zheng, E.S. Thian. *Materials Letters*, 172, 193–197, (2016).
3. A. Lakshmanan Pillai, G.R. Jinu, R. Elansezhian. *Int. J. Res. Appl. Sci. Eng. Technol.* 5(1), 22-30, (2017).
4. M. Edwin Sahayaraj, J.T. WinowlinJappes, I. Siva and N. Rajini. *Sci. Eng. Compos. Mater.* 23(3), 309 – 3014, (2014).
5. S. John Leon, J.T. WinowlinJappes and M. Edwin Sahayaraj. *J. Adv. Res. Dyn. Control Sys.* 10 (3), 1-6, (2018).
6. RajanVerma, Saurabhsharma, Dinesh Kumar. *Int. J. Eng. Res. Technol.* 6(3), 454 – 459, (2017).
7. AnkushkohLi, H. S Bains, sumit Jain, D Priyadarshi. *Mater. Sci. Res. india.* 14(2), 194-203, (2017).
8. J. Liu, H. Yu, C. Chen, F. Weng, J. Dai. *Optics and Laser in Engineering*, 93, 195–210 (2017).
9. V. K Bommala, K. G Krishna, V. T Rao. *J. Magnesium Alloys.* 7, 72–81(2019).
10. M. Valente, D. Marini, V. Genova, A. Quitadamo, F. Marra, G. Pulci. *J. Appl. Bio. Mater. Functinal Mater.* 17, 1–10 (2019).
11. J. Satish and K. G. Satish. *IOP Conferece Series: Mater. Sci. Engg.* 310, 1649–1655 (2018).
12. P. A Bajakke, V. R Malik, A. S Deshpande. *Materials and Manufacturing Process*, 34, 833–81 (2019).
13. NurettinSezer, ZaferEvis, Said Murat Kayhan, Aydin Tahmasebifar, MuammerKoc. *J. Magnesium Alloys*, 6 (1), 23-43, (2018).
14. Yang Chen, Jinhe Dou, Huijun Yu, Chuazhong Chen. *J. Biomater. Appl.*, 33(10), 1348-1372, (2019).
15. T. Judson Durai1, M. Sivapragash& M. Edwin Sahayaraj, Corrosion behaviour of Mg-Zr alloy in stimulated body fluid, *Int. J. Mech. Prod. Engg. Res. Develop.* 7 (6), 305 – 312, (2017).
16. Weigang Zhao, Song-Jeng Huang, Yi-Jhang Wu, Cheng-Wei Kan. *Metals*, 7(8), 293, (2017),
17. B.Selvam, P. Mari Muthu, R. Narayanasamy, V. Anandarkrishnan, K.S. Tun, M. Gupta, M. Kamaraj. *Mater. Des.* 58, 475-481, (2014).
18. M. Battabya, L. Veleva, N. Balu. *Int. J. Refract. Met. Hard Mater.*, 50, 210-216, (2015).
19. T. Judson Durai, M. Sivapragash& M. Edwin Sahayaraj, Effect of sintering temperature on mechanical properties of Mg-Zr alloy, *Int. J. Mech. Prod. Engg. Res. Develop.* 7 (5), 117 -122, (2017).
20. Ganesh Radhakrishnan, Anirudh P V, and Anujan Kumar S. *IOP Conf. Series: Mater. Sci. Eng.* 574, (2019) 012006, IOP Publishing doi:10.1088/1757-899X/574/1/012006.
21. M. Prakasam, J. Locs, K. Salma-Ancane, D. Loca, A. Largeteau, L. Berzina-Cimdina. *J. Funct. Biomater.*, 8(4), 44 – 59 (2017).
22. KhansaaSalman Haider, HashimHaiderHashim. *J. Mech. Eng. Res. Develop.* 43(1), 288-297, (2020).
23. J. Sathish, K.G Sathish. *IOP Conf. Series: Mater. Sci. Eng.* 310 (2018) 012130, IOP Publishing doi:10.1088/1757-899X/310/1/012130.
24. M. Paramsothy, X. Tan, J. Chan, R. Kwok, M. Gupta. *J. Alloys Compd.* 545, 12-18, (2012).
25. Maher Mounib, Matteo Pavese, Claudio Badini, Williams Lefebvre, HajoDieringa. *Adv. Mater. Sci. Eng.* Article ID 476079, 6 pages (2014), <http://dx.doi.org/10.1155/2014/476079>.
26. O.Sabokpa, A.Zarei-Hanzaki, H.R.Abedi. *Mater. Sci. Eng.: A*, 550, 31-38, (2012).

27. L. Chen and Y. Yao. *Acta Metallurgica Sinica (English Letters)*. 27(5), 762–774 (2014).
29. M. Abbasi, B. Bagheri, M. Dadaei, H. R Omidvar, M. Rezaei. *Int. J. Adv. Manuf. Technol.* 77, 2051–2058 (2015).
30. N. Anand and S. SenthilKumaran, *Mater. Res. Express*. 7 (3), (2020). <https://doi.org/10.1088/2053-1591/ab7d08>.
31. W. Liu, X. Wang, X. Hu, K. Wu, M. Zheng. *Mater. Sci. Eng. : A*, 683, 15–23, (2017).
32. S. Jayalakshmi, R. A. Singh, X. Chen, S. Konovalov, T. S. Srivatsan, S. Seshan, M. Gupta. *JOM*, 72, 2882–2891 (2020).
33. X. Gu, W. Cheng, S. Cheng, Y. Liu, Z. Wang, H. Yu, Z. Cui, L. Wang, H. Wang. *J. Mater. Sci. Technol.* 60, 77–89 (2020).
34. Yonghui Yan, Xiaoli Liu, HanqingXiong, Jun Zhou, Hui Yu, Chunling Qin, Zhifeng Wang. *Nanomaterials*, 10 (5), 947 (2020), <https://doi.org/10.3390/nano10050947>.
35. Ali Ercetin and DanilYurievichPimenov. *Materials*, 14, 4819 (2021), <https://doi.org/10.3390/ma14174819>.
36. J. Kumar, D. Singh, N. S. Kalsi, S. Sharma, C. I. Pruncu, D. Y. Pimenov, K. V. Rao, W. Kaplonek. *J. Mater. Res. Technol.* 9, 13607–13615 (2020).
37. S. Sharma, J. Singh, M. K. Gupta, M. Mia, S. P. Dwivedi, A. Saxena, S. Chattopadhyaya, R. Singh, D. Y. Pimenov, M. E. Korkmaz. *J. Mater. Res. Technol.* 12, 1564–1581 (2021).
38. Boyer H. E. and Gall T. L., 1985, *Metals handbook*, desk edition, USA.
39. AbhilashPurohit and AlokSatapathy, *Polym. Polym. Compos.* 29(9S), S1235–S1247 (2021).
40. Ben O'ShaughnessyDimitrios,VavylonisDimitriosVavylonis. *The European Physical Journal E*. 1(2), 159-177, (2000).
41. Zhang, Xuezhi, Li Fang, BojunXiong, and Henry Hu. *J. Mater. Eng. Perform.* 24(12), 4601-4611, (2015).
28. S.R.Yu and Z.Q. Huang. *J. Mater. Eng. Perform.* 23(10), 3480–3488 (2014).
42. Muhammad Rashad, Fusheng Pan, Huanhuan Hu, Muhammad Asif, ShahidHussain, Jia She. *Mater. Sci. Eng. : A*, 630, 36–44 (2015).
43. WeiweiLei,Taolue Wang, Hongxia Wang, Wei Liang. *J. Appl. Mater. Sci. Eng. Res.* 2(1), 1-3, (2018).
44. Y. Wu, K. Wu, K. Deng, K. Nie, X. Wang, M. Zheng, X. Hu. *Mater. Des.* 31(10), 4862–4865 (2010).
45. S. SilanTharakan, M. Sivapragash, E. Suneesh. *International Journal of Mechanical and ProductionEngineering Research and Development*, 9 (4), 355-362 (2019).
46. Mahdi Azizieh, ArshamNorouziLarki, Mehdi Tahmasebi, Mehdi Bavi, EhsanAlizadeh, HyoungSeop Kim. *J. Mater. Eng. Perform.* 27(1-2), 2010–2017 (2018).
47. T.Thirugnanasambandham,J.Chandradass, P. BaskaraSethupathi, M. LeenusJesuMartin. *Mater. Today: Proc.* 14 (2), 211-218 (2019).
48. SomayehAbazari, Ali Shamsipur, Hamid Reza Bakhsheshi-Rad, Ahmad Fauzi Ismail, Safian Sharif, MahmoodRazzaghi, Seeram Ramakrishna. *Materials*, 13(19), 4421 (2020); <https://doi.org/10.3390/ma13194421>.
49. Raman Singh, VijayaraghavanVenkatesh, Vinod Kumar. *Metals*, 8, 127, (2018), <https://doi:10.3390/met8020127>.
50. Chun Chiu and Hsu-Chieh Liu. *Metals*, 8, 424, (2018), <https://doi:10.3390/met8060424>.
51. DrahomírDvorský, JiříKubásek, Eva Kristianová, DaliborVojtěch. *Manuf. Technol.* 18(5), 737-741, (2018).
52. Kai Chen, Jianwei Dai, Xiaobo Zhang. *Corros. Rev.* 33(3-4), 101–117, (2015).